Bardossy A, Horning S.

Process-Driven Direction-Dependent Asymmetry: Identification and Quantification of Directional Dependence in Spatial Fields.

***Mathematical Geosciences* 2017**

DOI: https://doi.org/10.1007/s11004-017-9682-1

Mathematical Geosciences

Process-driven direction-dependent asymmetry: Identification and quantification of directional dependence in spatial fields

--Manuscript Draft--

Manuscript Number:	MATG-D-16-00046
Full Title:	Process-driven direction-dependent asymmetry: Identification and quantification of directional dependence in spatial fields
Article Type:	Original Research
Keywords:	Asymmetry; Rank-order geostatistics; Copula; Directional dependence; Reversibility
Corresponding Author:	Sebastian Hörning University Stuttgart Stuttgart, GERMANY
Corresponding Author Secondary Information:	
Corresponding Author's Institution:	University Stuttgart
Corresponding Author's Secondary Institution:	
First Author:	Sebastian Hörning
First Author Secondary Information:	
Order of Authors:	Sebastian Hörning
	András Bárdossy
Order of Authors Secondary Information:	
Funding Information:	DFG (GRK 1398) — Mr. Sebastian Hörning
Abstract:	Natural processes generate spatial fields which reflect their specific properties. In this paper the effect of the direction of processes on the resulting fields is investigated. This is done by extending the concept of reversibility used for time series to spatial processes. A novel copula based measure of asymmetry which is an indicator of directional dependence is defined. Contrary to traditional geostatistics where all points separated by a vector irrespective of its sign are considered here also the direction of the vector is taken into consideration, leading to differences in the dependence corresponding to the vector h and -h. The concept of directional dependence is independent of the scale of measurement, therefore the new measure of asymmetry is introduced using spatial copulas. It is a bivariate directional third-order moment based measure which can identify the direction in which the processes generating the spatial field acted. A statistical test to find the statistical significance is presented. The methodology is tested on a number of synthetic and observed cases. Precipitation and groundwater quality parameters obtained using numerical models are first investigated. Regular dense grids obtained by numerical simulations show good correspondence between properties of the modeled processes and the new measure introduced. Measured variables observed on sparse irregular networks show similar behavior as the theoretical examples. Mean flow directions in groundwater and advection directions of precipitation fields can be detected from single snapshots. As a further example dominating wind directions in the Sahara are found by investigating the digital terrain model. sebastian.hoerning@iws.uni-stuttgart.de

Mathematical Geosciences manuscript No.
(will be inserted by the editor)

Process-driven direction-dependent asymmetry: Identification and quantification of directional dependence in spatial fields

András Bárdossy · Sebastian Hörning

Received: date / Accepted: date

Abstract Natural processes generate spatial fields which reflect their specific properties. In this paper the effect of the direction of processes on the resulting fields is investigated. This is done by extending the concept of reversibility used for time series to spatial processes. A novel copula based measure of asymmetry which is an indicator of directional dependence is defined. Contrary to traditional geostatistics where all points separated by a vector irrespective of its sign are considered here also the direction of the vector is taken into consideration, leading to differences in the dependence corresponding to the vector h and $-h$. The concept of directional dependence is independent of the scale of measurement, therefore the new measure of asymmetry is introduced using spatial copulas. It is a bivariate directional third-order moment based measure which can identify the direction in which the processes generating

S. Hörning
University Stuttgart, Institute of Modeling Hydraulic and Environmental Systems, Department of Hydrology and Geohydrology
Tel.: +49-711-68569101
E-mail: sebastian.hoerning@iws.uni-stuttgart.de

A. Bárdossy
University Stuttgart, Institute of Modeling Hydraulic and Environmental Systems, Department of Hydrology and Geohydrology
Tel.: +49-711-68564663
E-mail: andras.bardossy@iws.uni-stuttgart.de

the spatial field acted. A statistical test to find the statistical significance is presented.

The methodology is tested on a number of synthetic and observed cases. Precipitation and groundwater quality parameters obtained using numerical models are first investigated. Regular dense grids obtained by numerical simulations show good correspondence between properties of the modeled processes and the new measure introduced. Measured variables observed on sparse irregular networks show similar behavior as the theoretical examples. Mean flow directions in groundwater and advection directions of precipitation fields can be detected from single snapshots. As a further example dominating wind directions in the Sahara are found by investigating the digital terrain model.

Keywords Asymmetry · Rank-order geostatistics · Copula · Directional dependence · Reversibility

1 Introduction

Observed spatial fields are often the results of complicated phyical, chemical and/or biological processes frequently known not in full detail. These processes act in time, but the time horizon can be very different, ranging from geological times for underground layers, through underground transport processes with time scales of months to years, to fast atmospheric processes with changes from hourly to minute scales. The processes whose realizations are observed are usually irreversible. This is a consequence of the second law of thermodynamics. This law implies that there is an asymmetry between past and future. The main research questions of this paper are:

Can the signs of an irreversible generating process be detected from a single spatial realization? Are a limited number of irregularly spaced observations sufficient to recognize the traces of an irreversible process?

Reversibility is a well known (but seldom used) concept in time series analysis. In Lawrance and Lewis (1985) and Lawrance (1991) a time series such as a streamflow record is defined to be irreversible (or directional) if its properties depend on the direction of time. It is reversible if its properties do not depend on the direction of time. The first approaches to detect directionality are via graphical inspection of the time series which can often reveal irreversibility. There is some literature on testing reversibility in time series, for example using cumulants (Giannakis and Tsatsanis, 1994). As Gaussian time series are reversible, these tests were frequently used to test Gaussianity of time series. Other methods are available for testing Markov chains for reversibility, for example in Steuber et al (2012).

In spatial statistics, reversibility is seldom utilized as the time series definition cannot simply be extended to higher dimensional spaces. The main reason for this is that space has no single direction. One can move backwards in space but not in time. A further problem is that most geostatistical problems are dealing with sparse irregularly spaced observations thus directionality cannot be recognized by simply looking at the data. As there is no definition there are also no measures to examine directionalities in spatially distributed variables. Finally, tools that enable modeling of spatial irreversibility are not available.

In general, one could say that a lack of reversibility means asymmetry in the dependence. Some concepts of asymmetrical dependence were already developed in geostatistics. Basically, asymmetry describes the deviation from the symmetrical, for example from the frequently used traditional Gaussian case. Different studies show that asymmetry in the dependence has a significant influence on the spatial variable of interest as well as on related processes and variables. For example, Zinn and Harvey (2003) show that an asymmetric dependence structure of hydraulic conductivities leads to significantly altered transport behavior. In Guthke (2013) several natural parameters like surface elevations are shown to have an asymmetric dependence. Bárdossy (2006) shows that different groundwater quality parameters exhibit an asymmetrical thus non-Gaussian spatial dependence structure. In Haslauer et al (2012) the authors show that the Borden aquifer in Canada can be modeled using an asymmetrical thus non-Gaussian spatial copula.

Some specific processes like transport, advection, or erosion can exhibit certain directions in which the processes act. Such processes can additionally lead to asymmetries that are distinguishable in different directions. Such directional asymmetries are the focus of this paper. New geostatistical tools are presented which are able to identify and to quantify directionality in spatially distributed variables. Therefore, the time series definition of reversibility is extended to

higher dimensions and a weak form of spatial reversibility, the directional independence, is introduced. Directional copulas are used for statistical testing of directional independence. Furthermore, a direction-dependent asymmetry function is introduced that enables quantification. Different examples that are expected to exhibit directionality are investigated using the new tools. The examples range from synthetical flow and transport experiments over surface elevation data to precipitation modelling and measurements.

This paper is divided in four parts. After the introduction, the basic definition of reversibility in time series analysis is presented and extended to a spatial context. The theory part also covers a review of rank-order geostatistics as well as the basics of spatial copulas as the new introduced directional asymmetry function is based on copulas which are rank-order based geostatistical tools. The third section shows different examples using theoretical and observed spatial variables to demonstrate the applicability and the usefulness of the new measure. Finally, conclusions are drawn in section four.

2 Theory

In this section first the time series notion of reversibility is recalled and subsequently extended to higher dimensional spaces. A weak form of spatial reversibility, the directional dependence, is introduced next. As reversibility and irreversibility are properties of the dependence they can be measured and statistically tested independently of the one dimensional marginal distributions. Thus the investigations are carried out in the copula space. The basics of empirical rank-order geostatistics, as well as the basics of spatial copulas, are reviewed followed by a short review of the classical rank-order geostatistical measures of dependence.

2.1 Reversibility

Reversibility is well known in time series analysis (Lawrance and Lewis, 1985; Lawrance, 1991; Giannakis and Tsatsanis, 1994), however, it is hardly utilized in spatial statistics. A discrete stationary time series $Z(t)$ is reversible if its statistical properties do not depend on the direction of time. Formally

$$Z(t), Z(t+1), \ldots, Z(t+k-1) \stackrel{d}{=} Z(t+k-1), Z(t+k-2), \ldots, Z(t) \quad (1)$$

where $\stackrel{d}{=}$ means identically distributed for any k and time t. This definition can be extended to a spatial context in different forms. The simplest definition would be to require reversibility for the process restricted to any single straight line in the space. Another more general definition is:

Definition: A spatial random field $\mathbf{Z}$ in domain $\mathcal{D}$ in n dimensional Euclidian space is fully reversible if for any points $\mathbf{x_1}, \ldots, \mathbf{x_n}$ in $\mathcal{D}$, and any isometric transformation $T(x)$ such that $T(\mathbf{x_1}), \ldots, T(\mathbf{x_n})$ is in $\mathcal{D}$, the multivariate distributions

$$Z(\mathbf{x_1}), \ldots, Z(\mathbf{x_n}) \stackrel{d}{=} Z(T(\mathbf{x_1})), \ldots, Z(T(\mathbf{x_n})) \quad (2)$$

where the isometric transformation T is by definition preserving the point inter distances

$$d\left(T(\mathbf{x_i}), T(\mathbf{x_i})\right) = d(\mathbf{x_i}, \mathbf{x_j}) \quad (3)$$

with d denoting the Euclidian distance.

In one dimension isometric transformations are translations. In higher dimensions they consist of a lot of additional transformations such as rotations, in addition to translations. Thus a weaker form of reversibility using only two

points is more convenient. We call Z directionally independent if it is as the special case $k = 2$:

Definition: A stationary spatial random field Z in domain $\mathcal{D}$ in n dimensional Euclidian space is directionally independent if for any points $\mathbf{x_1}, \mathbf{x_2}$ in $\mathcal{D}$

$$Z(x_1), Z(x_2) \stackrel{d}{=} Z(x_2), Z(x_1) \tag{4}$$

This second definition of directional independence requires weaker conditions than full reversibility, thus if Z is not directionally independent then it is also not fully reversible. It is important to notice that all concepts of reversibility reflect properties of the dependence structure. For any increasing monotonic transformation of the process the transformed and the original have the same reversibility or irreversibility properties. Thus one can investigate reversibility with a unified marginal, for example taking the copula of the distribution. This path is followed in this paper and for this a short overview of copulas is first given.

2.2 Rank-order geostatistics and spatial copulas

Journel and Deutsch (1997) first proposed the use of rank-order geostatistics. They suggested to transform the data into a common $[0, 1]$ interval. They showed that this transformation preserves the spatial ranks of the data and that any Kriging and stochastic simulation approach can be perfomed in this transformed space. Bárdossy (2006) extended the idea of rank-order geostatistics by using copulas to describe spatial dependence. Using copulas, different kinds of dependencies for different quantiles of values, that is, asymmetry

of the spatial variable of interest, can be taken into account. Copulas are a special class of multivariate distribution functions with uniformly distributed univariate marginal distributions defined on the interval $[0,1]$

$$C : [0,1]^n \rightarrow [0,1] \tag{5}$$

Sklar's theorem (Sklar, 1959) can be used to describe any multivariate distribution function $F(x_1,\ldots,x_n)$ with the help of a copula

$$F(x_1,\ldots,x_n) = C(F_{X_1}(x_1),\ldots,F_{X_n}(x_n)) \tag{6}$$

where $F_{X_i}(x_i) = u_i$ with u_i denoting a uniformly distributed variable and $i = 1\ldots n$. An advantage of using rank-order geostatistics including the use of copulas is that the marginal distributions can be fitted independently from the multivariate dependence structure and that any monotone transformation of the marginals would not change the multivariate dependence in rank space, that is, the copula. Further details on copulas can be found in Nelson (1999).

Copulas can be used to describe spatial dependence. For a stationary spatial process Z with the univariate marginal being F_Z the bivariate spatial copula corresponding to a vector h is defined by

$$C_h(u,v) = P\left(F_Z(Z(x+h)) < u, F_Z(Z(x)) < v\right) \tag{7}$$

The density of this copula is denoted by $c_h(u,v)$. For further details on copulas in geostatistics the interested reader is refered to Bárdossy (2006).

2.3 Classical measures of dependence and direction-dependent asymmetry

Instead of investigating the spatial process with its specific univariate marginal distribution the process $U(x) = F_Z(Z(x))$ is considered. Here $F_Z(Z(x))$ is the

univariate marginal of Z. This newly defined U has uniform one dimensional marginals.

In traditional geostatistics, either the covariance function or the experimental semi-variogram are used to describe the dependence of pairs of points separated by a distance vector **h**. In rank-order geostatistics the rank correlation function is used

$$R(h) = 12E[(U(s) - 0.5)(U(s+h) - 0.5)] \tag{8}$$

Here s denotes a spatial coordinate, h denotes a distance vector, 0.5 is the mean and $\frac{1}{12}$ is the variance of the uniform distribution. The advantage of using the rank correlation function in comparision to the variogram or covariance is that it is not sensitive to outliers and that all monotone dependencies are measured. However, the rank correlation is still second a order moment, that is, it describes the average dependence over the whole range of quantiles.

To overcome this drawback the asymmetry function can be used. In Guthke (2013) the asymmetry function is defined as

$$A(h) = E[(U(s) + U(s+h) - 1)^3] \tag{9}$$

This can be written using the density of the bivariate spatial copula $c_h(u, v)$ describing the dependence corresponding to the separation vector h

$$A(h) = \int_0^1 \int_0^1 (u + v - 1)^3 c_h(u, v)\, dv\, dv \tag{10}$$

This asymmetry function defined in Eqs. (9, 10) is able to express the different strengths of dependence for different quantiles and different distance classes. Hence, it goes one step beyond the Gaussian assumptions (second order moment) as the dependence for different quantiles of values is distin-

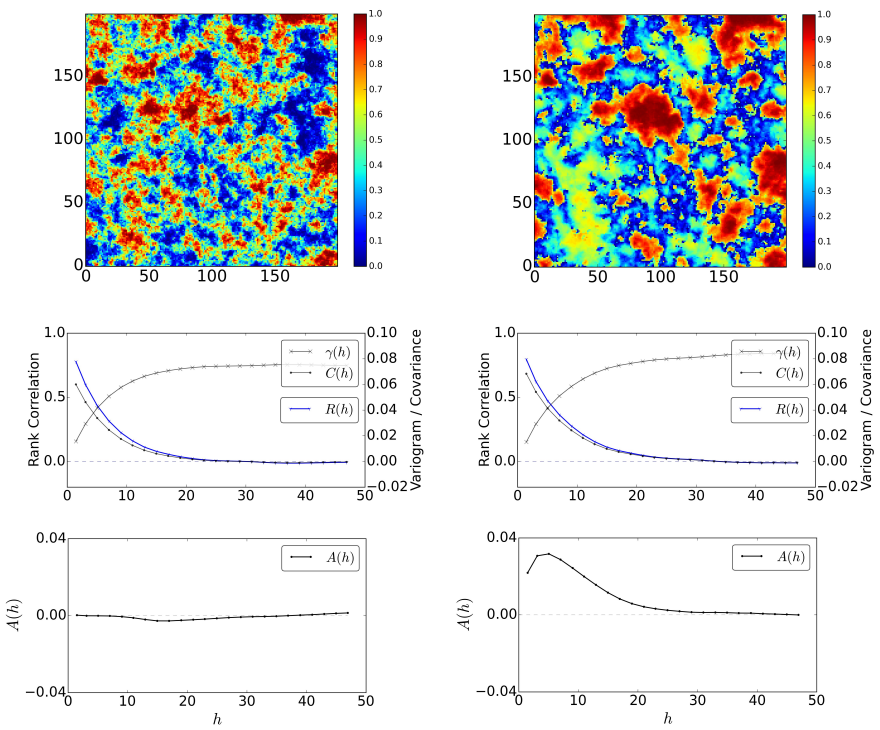

Fig. 1 This figure shows a Gaussian random field (left) and a non-Gaussian random field (right) with corresponding variogram $\gamma(h)$, covariogram $C(h)$, rank correlation function $R(h)$, and asymmetry function $A(h)$.

guished and not averaged. Fig. 1 shows two common (i.e. they share the same random path for the sequential simulation) spatial random fields (Guthke and Bárdossy, 2012) that share almost exactly the same variogram/covariogram/rank correlation function but clearly exhibit different spatial patterns. Those differences cannot be captured using an average description of the dependence over the whole range of quantiles. However, the above defined asymmetry function is able to identify the different dependence structures. It can be seen that the asymmetry is almost zero in the left field while it is positive for small separation distances in the right field. More examples and details on interpretation can be found in Guthke (2013). If a spatial random field is asymmetric according to the definition in (10), it is assumed to be directionally indepen-

dent. In contrast directional dependence means that the spatial dependence corresponding to a vector h is different from that corresponding to $-h$. This property means that the copula density is not symmetrical

$$c_h(u,v) \neq c_h(v,u) \tag{11}$$

A possible measure for this can be defined as

$$A_d(h) = E[(U(s) - U(s+h))^3] \tag{12}$$

Another way of expressing this is

$$A_d(h) = \int_0^1 \int_0^1 (u-v)^3 c_h(u,v)\, dv\, dv \tag{13}$$

Note that by definition the above defined asymmetry function depends on the direction of the vector h

$$A_d(-h) = -A_d(h) \tag{14}$$

This asymmetry function can be calculated from observed data using the bivariate empirical spatial copula, or directly as

$$A_d^*(h) = \frac{1}{N(h)} \sum_{x_i - x_j \approx h} (F(Z(x_i) - F(Z(x_j)))^3 \tag{15}$$

where $x_i, i = 1, \ldots n$ are the observation points, $N(h)$ is the number of pairs such that x_i and x_j are separated by a vector which is approximately h. The calculation is very similar to the calculation of the experimental variogram, with two major differences: (i) The direction of the vector h is taken into account, and (ii) The value of the empirical distribution function is used for the calculation.

The assumption of directional independence can be tested using observed data. The assumption is that the distributions of the empirical copula corresponding to a vector h are such that (u_i, v_i) and (v_i, u_i) do not differ significantly. In order not to use data twice this can be formulated so that the distributions

$$(u_i, v_i) \text{ with } u_i < v_i \text{ and } (v_i, u_i) \text{ with } u_i > v_i \tag{16}$$

can be regarded as identical. Fig. 2 shows an empirical copula corresponding to a vector h and its mirror image (which is the copula corresponding to the vector $-h$). In case of directional independence the two sets above the diagonal should belong to the same distribution.

Directional independence can be tested by comparing the above two distributions both defined on the triangle formed above the diagonal of the unit square. Kolmogorov-Smirnov tests can be used for this purpose.

Another possibility is to restrict the comparison to the upper left corner ($[0, \frac{1}{2}] \times [\frac{1}{2}, 1]$) as indicated in Fig. 2. This square provides the strongest contribution to the asymmetry. An advantage of this choice is that the number of points falling in this square for the original and the mirrored copula is the same. Here a χ-square test is a good candidate for testing. A possible disadvantage of restricting the test to the upper left corner is that, in the case of strong dependence, the square is sparsely populated.

3 Examples

In this section, examples are used to demonstrate how processes can lead to directional asymmetries and how these asymmetries can be indentified and quantified. The examples use regularly sampled observed cases (topography), numerically simulated cases (contamination and precipitation), and irregularly

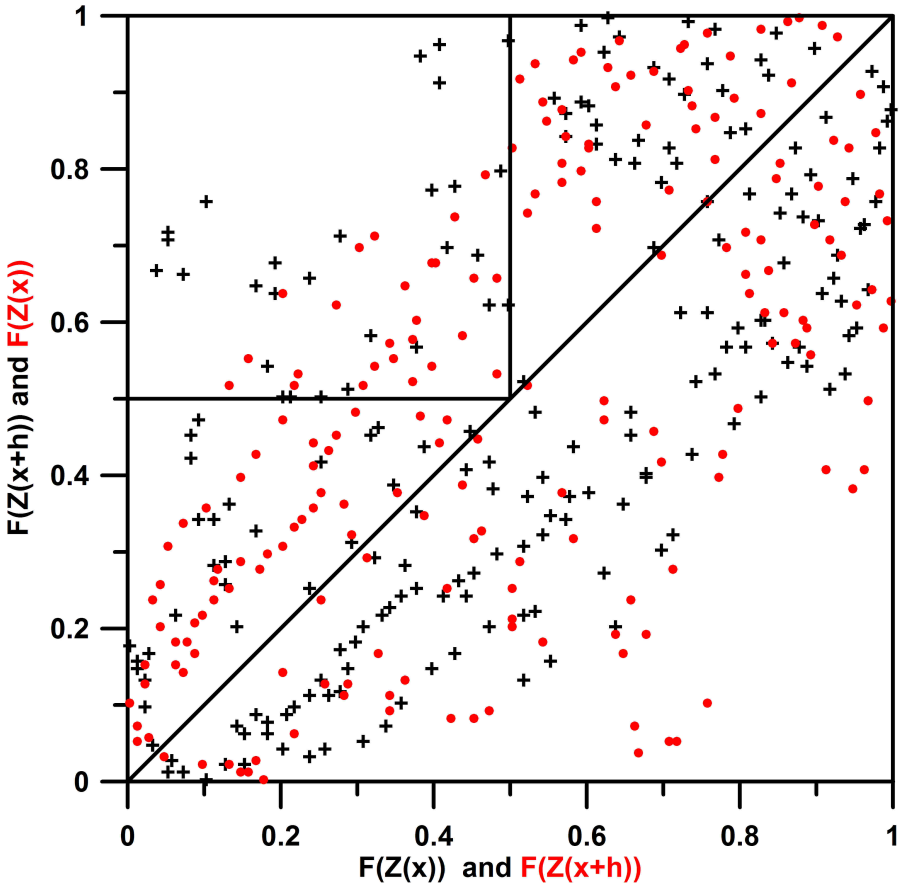

Fig. 2 Empirical spatial copulas corresponding to a vector h (black crosses) and to the vector $-h$ (red circles). In the case of directional independence the distribution of the black crosses and the red circles above the diagonal should be the same.

and sparsely sampled observed cases (precipitation). In all cases the asymmetry function was calculated for different directions and for each of the above described cases a χ-square test is applied to test for statistical significance.

3.1 Gaussian random fields

This first example aims to demonstrate that directional dependence is significantly non-Gaussian and that it is not to be confused with classical anisotropy. Therefore, 100 isotropic Gaussian random fields as well as 100 anisotropic

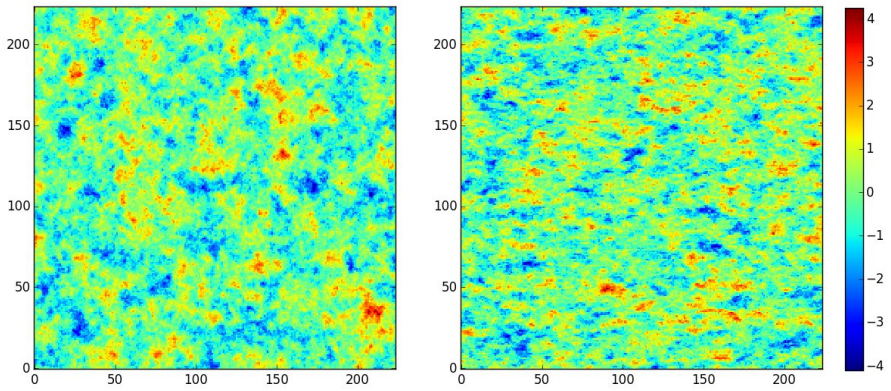

Fig. 3 Left: Isoptropic Gaussian random field. Right: Anisotropic Gaussian random field.

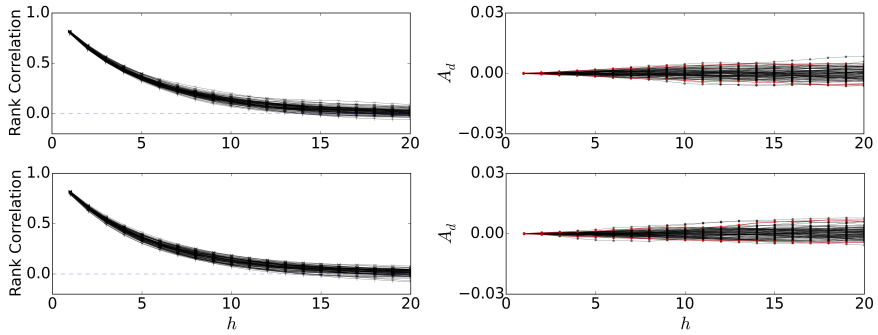

Fig. 4 Rank correlation and directional asymmetry functions according to the 100 isotropic Gaussian random fields. The upper plot corresponds to the horizontal direction the lower plot to the vertical direction. The red lines denote the 95% confidence interval.

Gaussian random fields are simulated. The isotropic fields are simulated on a regular 224×224 grid using an exponential variogram with an effective range of 15 pixels. The anisotropic fields are also simulated on a regular 224×224 grid using an exponential variogram with an effective range of 15 pixels in the horizontal direction and an exponential variogram with an effective range of 8 pixels in the vertical direction. Two simulated fields are shown in Fig. 3. For all simulated fields the directional asymmetry functions as well as the rank correlation functions are calculated considering two directions, horizontal and vertical. They are shown in Fig. 4 and Fig. 5, respectively.

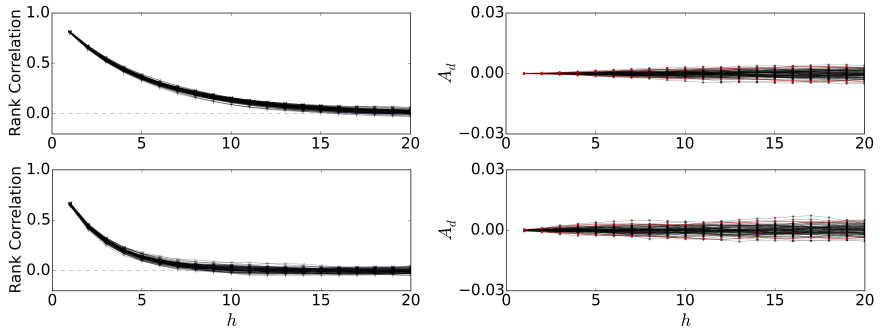

Fig. 5 Rank correlation and directional asymmetry functions according to the 100 anisotropic Gaussian random fields. The upper plot corresponds to the horizontal direction the lower plot to the vertical direction. The red lines denote the 95% confidence interval.

Table 1 Percentage of Gaussian random fields for which directional independence is rejected on the 95% level. v denotes the vertical direction, h denotes the horizontal direction.

	$h_1 = 3$ h	$h_1 = 3$ v	$h_2 = 6$ h	$h_2 = 6$ v	$h_3 = 9$ h	$h_3 = 9$ v
isoptropic	4	3	3	5	4	3
anisotropic	3	5	4	3	5	4

In the isotropic case it can be seen that the rank correlation functions as well as the directional asymmetry functions behave similar for both directions. The directional asymmetry increases with decreasing rank correlation. The anisotropic case shows basically the same behavior. However, it can be seen that the correlation lenght is shorter in the vertical direction. As a result the directional asymmetry in the vertical direction increases already for shorter separation distances.

To test whether the calculated directional asymmetries are significant all simulated fields are tested for directional independence considering the two directions (horizontal and vertical) and three distances ($h_1 = 3$, $h_2 = 6$, $h_3 = 9$). Therefore, the above described χ-square test is applied. The proportions of fields for which directional independence is rejected on the 95% level is shown in Table 1. The results of the χ-square test show that Gaussian random fields are directional indepedent. Only about 5% of all cases are rejected by the χ-

square test. This is approximately the proportion which one would randomly expect. Thus, directional asymmetry and with that directional dependence is not a significant property of Gaussian fields. It is important to note that this holds for both the isotropic as well as the anisotropic case. Thus, it can be concluded that directional dependence is neither Gaussian nor a special kind of anisotropy and must therefore not be confused with it.

3.2 Synthetical flow and transport example

In order to demonstrate a process that obviously leads to directional asymmetry a synthetical flow and transport example is used. A conservative tracer is injected into a heterogeneous depth-averaged aquifer and the concentration of tracer is the spatial variable of interest. The advantage of this example is that the distribution of tracer is known exactly over the whole domain and that the directional dependence, respectively directional asymmetry, is already visually recognizable.

The general flow set-up is as follows. The domain length is 0.8 m in the x direction and 1 m in the y direction, discretized into grid cells of 1×1 cm. The upper and lower boundaries share no-flow conditions. Flow from left to right is enforced by prescribed heads of 25 cm and 15 cm, respectively. The underlying hydraulic transmissivity field is unconditionally simulated using fast Fourier transformation for regular grids (Wood and Chan, 1994; Wood, 1995; Ravalec et al, 2000). It exhibits a Gaussian spatial dependence structure with an exponential variogram without nugget and an effective range of 24 cm. The transmissivities follow a lognormal univariate marginal distribution with a mean $log_{10}T$ of -2.9 and a $log_{10}T$ variance of 0.189. A conservative tracer is injected at several random locations and the flow and transport simulation is performed. Figure 6 shows the resulting tracer concentration field 30 hours

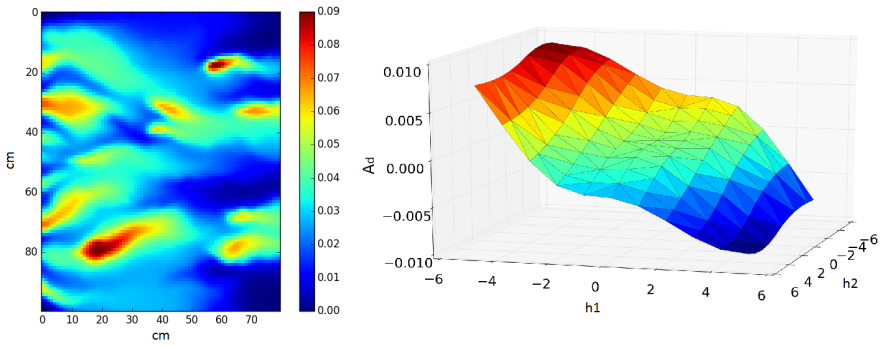

Fig. 6 Tracer concentration $[\frac{kg}{cm^3}]$ field at time step $t = 30\ h$ (left) with corresponding 2-dimensional directional asymmetry function (right). h_1 and h_2 are the components of the separation vector h.

after injection. From this concentration field the corresponding directional asymmetry is calculated and also shown in Fig. 6. The mean flow direction of solute can clearly be seen in the concentration field. This concentration field is obviously directional dependent with respect to the mean flow direction which can also be observed from the directional asymmetry function. The above described χ-square test is applied to test for directional independence using a significance level of $\alpha = 1\%$. The test shows that the concentration field is significantly directional dependent in flow direction while it is directional independent perpendicular to the mean flow direction. This can also be observed from the directional asymmetry function which is almost zero perpendicular to the main flow direction. The interpretation of the directional asymmetry in this example is straight forward: it is likelier to find a low value going from left to right, that is, going in the mean flow direction, and vice versa. From a physical point of view this finding makes sense as advection acts from left to right diluting the solute in this direction.

To demonstrate that directional asymmetry can also be detected from irregularly spaced point measurements the example is slightly changed. The concentration field shown in Fig. 6 is randomly sampled at 1000 locations.

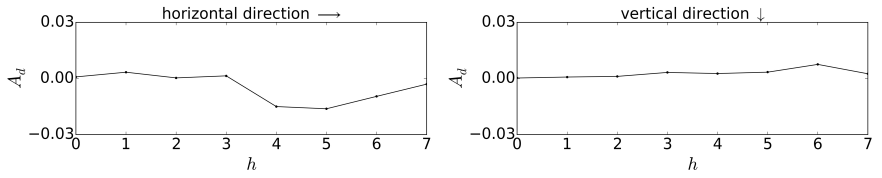

Fig. 7 Asymmetry functions corresponding to the irregularly sampled concentration data.

These synthetical measurements are then used to determine the directional asymmetry function. As the observations are irregularly spaced and there are only a limited number of oservations the directional asymmetry function has to be calculated on a coarser resolution. That means distance classes and direction (angle) classes have to be defined. Here only the two main directions, horizontal and vertical are considered. A tolerance range of $\pm 25°$ is considered. The resulting directional asymmetry functions are shown in Fig. 7. It can be seen that the asymmetry functions obtained from the irregularly spaced observation are comparable to the one obtained from the entire concentration field. The asymmetry is almost zero perpendicular to the main flow direction while it is negative in the flow direction. This demonstrates that directional dependence can also be detected from a single snapshot that consist of irregularly space point observations only. This is quite encouraging as this is the usual case for real world data.

3.3 CRM2 precipitation data

In this example CRM2 (Ban et al, 2014, 2015) precipitation data is investigated. CRM2 denotes convection-resolving model with a horizontal resolution of 2.2 km simulated for a 6 yearlong period from $1998 - 2004$ on an extended Alpine domain with hourly resolution. The CRM2 model improves the simulation of precipitation over the Alps, however the main advantage of this model in terms of a spatial investigation is the detailed resolution. The full model

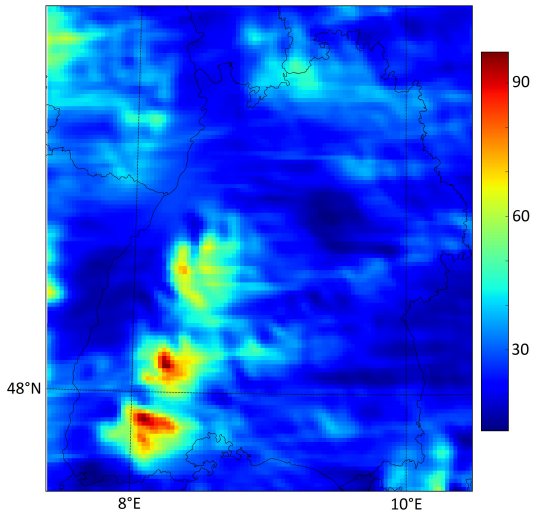

Fig. 8 CRM2 precipitation field aggregated to pentad temporal resolutions corresponding to January 1st - 5th, 1998.

covers an area of 1100 km $\times$ 1100 km but here only the area of the federal state of Baden-Württemberg is extracted and different temporal resolutions are considered. Therefore, the hourly data are extracted and aggregated to daily, pentad, and monthly temporal resolutions. This results in 2546 daily precipitation fields, 510 pentad precipitation fields, and 84 monthly precipitation fields. An example CRM2 precipitation field corresponding to a five days temporal aggregation is shown in Fig. 8.

For all those aggregated precipitation fields with less than 20% zero values the directional asymmetry functions and the rank correlation functions are calculated considering two directions (S-N and SW-NE). They are shown in Fig. 9 and 10, respectively. It can be seen that for all aggregations the south-west to north-east direction exhibits higher asymmetries than the south to north direction. Looking at the rank correlation functions, the south north direction exhibits larger correlation lengths especially in the monthly aggregation compared to the south-west north-east direction, indicating anisotropy. However, as already stated the asymmetry in south north direction is smaller

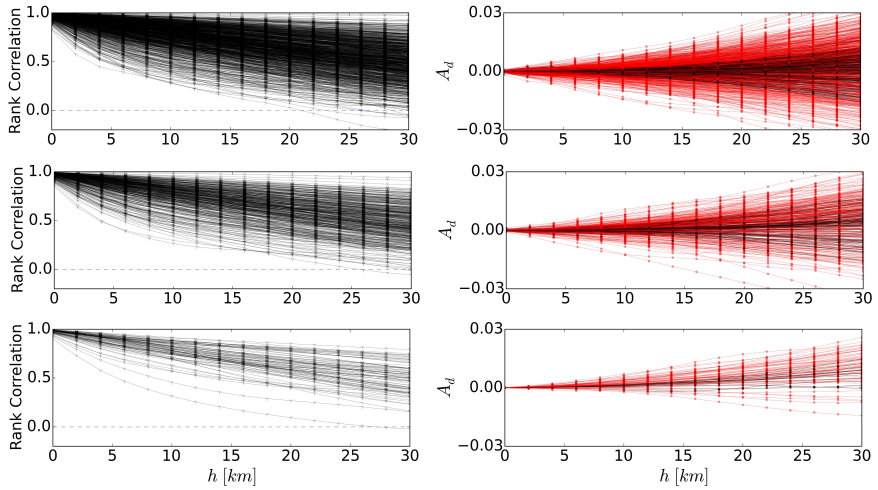

Fig. 9 Rank correlation and directional asymmetry functions with direction going from south to north corresponding to the daily (upper), five days (middle), and monthly (lower) aggregation. The red lines correspond to the cases with significant directional dependence.

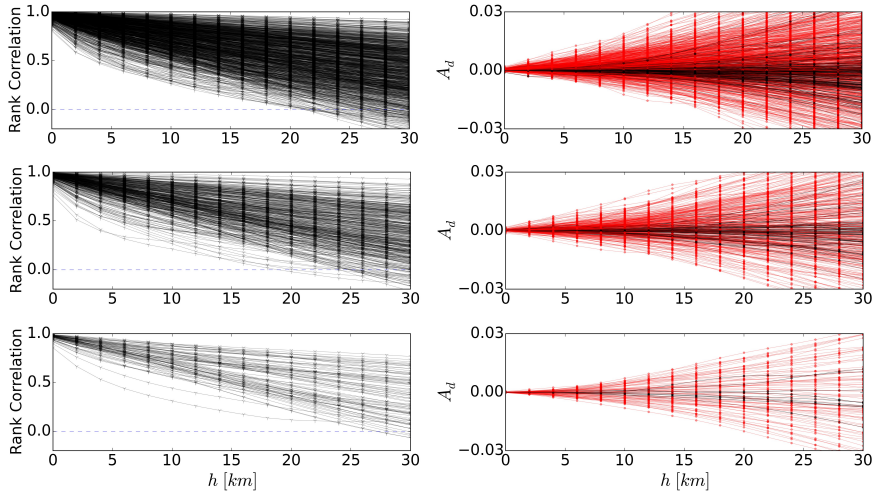

Fig. 10 Rank correlation and directional asymmetry functions with direction going from south-west to north-east corresponding to the daily (upper), five days (middle), and monthly (lower) aggregation. The red lines correspond to the cases with significant directional dependence.

Table 2 Percentage of precipitation fields for which directional independence is rejected on the 95% level. Different temporal aggregations and different directions are considered.

Direction	monthly 6 km	5-days 6 km	daily 6 km	monthly 12 km	5-days 12 km	daily 12 km
W-E	10	9	10	10	11	12
S-N	10	4	5	10	7	6
SW-NE	24	28	27	28	28	26
NW-SE	41	43	39	48	47	46

than in south-west north-east which indicates that asymmetry and anisotropy express different properties of the generating process.

To test for directional independence χ-square test is applied. Therefore, four directions and two distances are considered. The directions are south to north (S-N), west to east (W-E), south-west to north-east (SW-NE), and north-west to south-east (NW-SE). The distances are $h_1 = 6\ km$ and $h_2 = 12\ km$. The proportions of fields for which directional independence is rejected on the 95% level are shown in Table 2. As some fields exhibit significant directional dependence for different directions only the most significant direction is considered. This is a frequent case, as directions with a sharp angle to the advection direction also exhibit some directional dependence. Note that the precentages do not sum up to one as for some fields the assumption of directional independence is not rejected. Further, it can be seen that the NW-SE direction shows the highest amount of significant fields for all aggregations while the S-N direction shows the smallest amount of significance. In the federal state of Baden-Württemberg the main wind directions are W-E, SW-NE, and NW-SE. These winds could be the driving forces for the directional asymmetries, that is, the process that makes the precipitation fields irreversible in that directions. Thus, the significant directional dependence can be seen as a sign of a W-E dominated wind system, which is actually prevailing in south-west Germany.

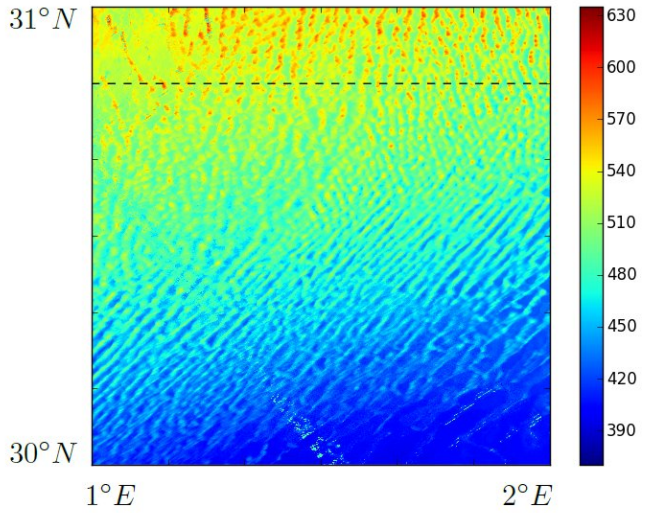

Fig. 11 Topographic map of the Sahara desert in Algeria with 80 m spatial resolution. The dotted line marks the location of the extracted cross section.

3.4 Topography of the Sahara

In this example the surface elevation of the Sahara desert is investigated by using the data obtained from a digital terrain model. The area of interest is located in Algeria (from $30°N$ $1°E$ to $31°N$ $2°E$) and consists mainly of sand desert forming large sand dunes. The corresponding topographic map is shown in Fig. 11. The genesis of these sand dunes is predominantly driven by wind. For this particular region the main wind direction is from east to west as it is located at the boundary of the northeasterly trade winds zone. Due to these winds sand begins to pile up and dunes can form. If the wind is steady and strong enough it continues to move sand to the top of the pile until the pile is so steep that it collapses (Balmforth and Provenzale, 2001; Tsoar, 2001). Thus, the dune's leeward side exhibits a steep slope while its windward side exhibits a flatter slope. A cross section from west to east (marked by the dotted line in Fig. 11) is extracted from the digital elevation map. Fig. 12 shows the resulting

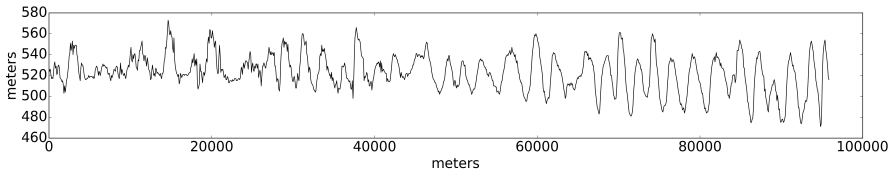

Fig. 12 Elevation cross section of the Sahara desert corresponding to the dotted line in Fig. 11.

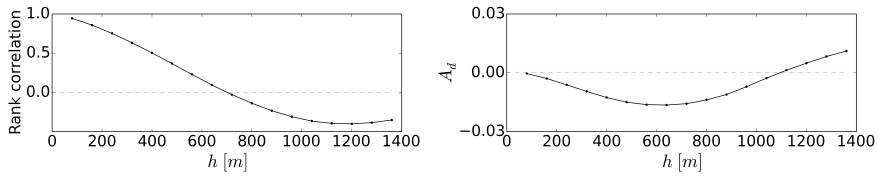

Fig. 13 Rank correlation and directional asymmetry function according to the topographic cross section of the Sahara.

elevation profile. A first visual inspection of this cross section already shows the above described features. It can be seen that the slopes at the west sides of the dunes are steeper than at the east sides which are generally rougher.

Figure 13 shows the rank correlation function and the directional asymmetry function calculated for the cross section shown in Fig. 11. The orientation of the distance vectors used for the calculation of the directional asymmetry is west to east (W-E). It can be seen that the rank correlation becomes negative for separation distances bigger than 700 m. The directional asymmetry is negative for separation distance up to 1100 m, getting positive afterwards. This negative

Directional dependence of the cross section is tested using the above described χ-square test. Three separation vectors ($h_1 = 320m$, $h_2 = 480m$, $h_3 = 640m$) with W-E orientation are considered. The scatter plots, the ranked scatter plots, and the empirical directional copula densities corresponding to these vectors are shown in Fig. 14. These directional copulas are tested for directional independence. For all three separation vectors the χ-square test

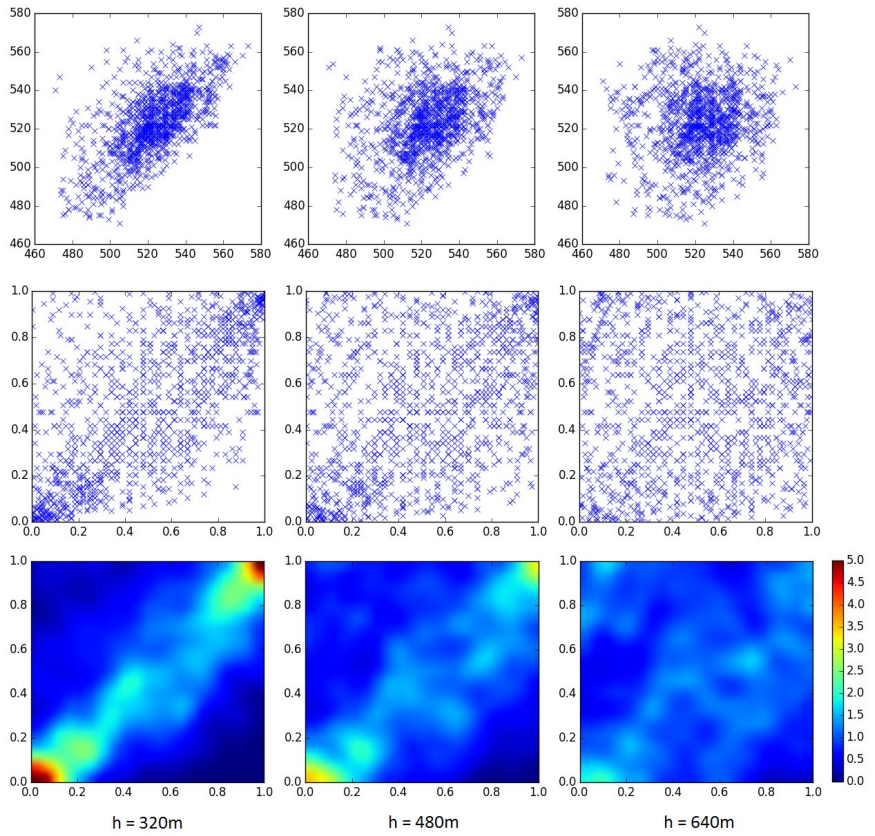

Fig. 14 Upper: Scatter plot of elevations. Middle: Scatter plot of ranked elevations. Lower: Empirical directional copula densities. All calculated from the cross section shown in Fig. 12 for given separation vectors with W-E orientation.

indicates that the directional copula densities are significantly directional dependent at a 95% level. That means the test rejected that the directional copulas are directional independent.

According to the directional asymmetry function, all empirical directional copula densities share a negative directional asymmetry in the W-E direction. At a first glance this seems to be implausible as all copulas exhibit higher densities in the uppermost left part indicating postive asymmetry. However, having a closer look at the copula densities it can be seen that the overall denisties are higher in the lower right triangles than in the upper left triangles.

Even though there are low densities in the lowermost right part (which would have a strong negative contribution to the directional asymmetry function) the higher densities in the lower right triangle outweigh the positiv asymmetry. Thus, the overall directional asymmetry becomes negative. This behavior can be explained having a closer look at the elevation profile. One can see that there are steep slopes on the west sides of the sand dunes while the slopes on the east sides are flatter. The steep slopes lead to the positive component while the flatter east sides lead to the negative asymmetry. As the directional asymmetry function is an integral measure it is favourable to investigate also the empirical directional copula densities as they allow a more detailed investigation.

3.5 Irregularly spaced observations of daily precipitation

Directional dependence can sometimes be seen by eye looking at a completely filled image. This is very unlikely if observations are available only on a limited number of usually irregularly spaced locations. The calculation of the asymmetry function and the statistical testing of the empirical spatial copula does not require a regular and complete dataset. The calculation of the asymmetry using irregular grids was already considered in the flow and transport example shown in Fig. 6. Here a large number of observed data sets are considered. In order to have a sufficiently large number of cases daily precipitation measured in Baden-Württemberg and Rhineland-Palatinate at up to 474 and 239 locations respectively, in the time period of 1961-2001 were used. Days with at least 1 mm average precipitation and with less than 20 % of dry stations were used. Results obtained for the CRM2 precipitation data indicate that directional dependence can be expected for these observed data too.

For Baden Württemberg 2223 out of the selected 4351 days showed directional dependence on the 95% level. This result was obtained for vectors of

the length of 20 km and 8 directions. The most frequent dominant direction with significant asymmetry was SW-NE.

1344 out of the 3780 days selected for Rhineland-Palatinate showed directional dependence on the 95% level. The same vectors were used for the calculation as for Baden Württemberg. The most frequent dominating direction was W-E which corresponds to the dominating geostrophic wind direction.

It is important to note that the advection is not homogeneous on single days, therefore there are many days where directional dependence could not be detected. Despite this the number of days with directional dependence is far above the 5% what one would randomly expect. The CRM2 results show more frequent directional dependencies than observations, which may be due to certain simplifications of the model, and to the larger set of points used for the calculations. Further the spacing of the data did not allow the calculation of the asymmetry for short distances as in the CRM2 example.

Figure 15 shows as an example precipitation on January 10, 1993 as measured at 175 locations in Rhineland-Palatinate. From the scattered points it is difficult to see a directional dependence. Figure 16 shows the asymmetry functions calculated for four directions (note the other four are the same but with opposite sign). A_d values corresponding to the W-E direction are the biggest in magnitude while the orthogonal direction N-S shows the smallest values. The two diagonals are in between. Except for N-S the three other directions show significant directional dependence. This is a sign of a W-E dominated process.

4 Discussion and conclusion

In this paper the concept of reversibility of time series was extended to spatial processes. The simplest form of spatial reversibility is directional inde-

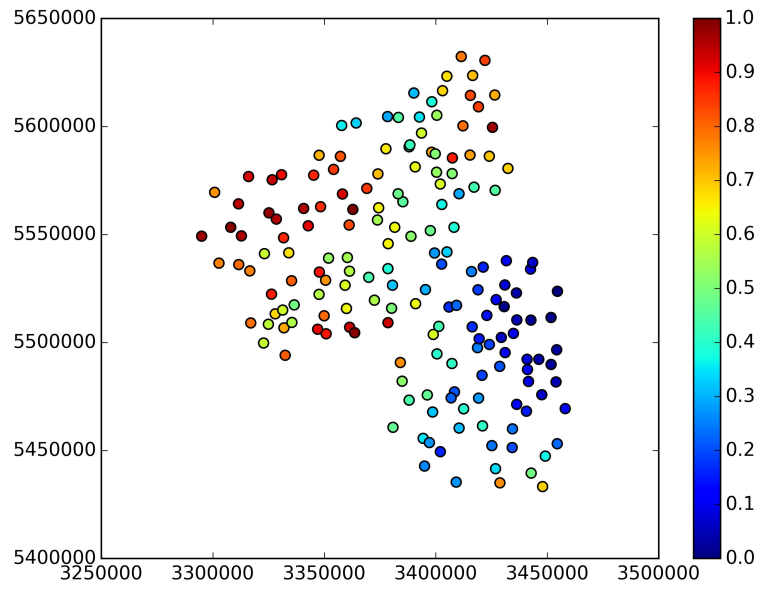

Fig. 15 175 daily precipitation values (in rank space) measured on January 10, 1993.

pendence. Directional independence does not depend on the one dimensional marginal distribution of the process, it is a property of the spatial copula. In order to measure directional dependence a new direction-dependent asymmetry function was introduced. This function measures directional dependence based on a third order statistics of the bivariate experimental copulas. Statistical tests were introduced to assess statistical significance of directional dependence.

A numerical example based on simulated Gaussian random fields was used to demonstrate that Gaussian fields are directional independent, which means they do not exhibit significant directional asymmetries. Further, it was shown that directional dependence is a different property than anisotropy. Examples obtained using numerical simulation of processes for which advection plays a central role, namely groundwater transport of polution and precipitation sim-

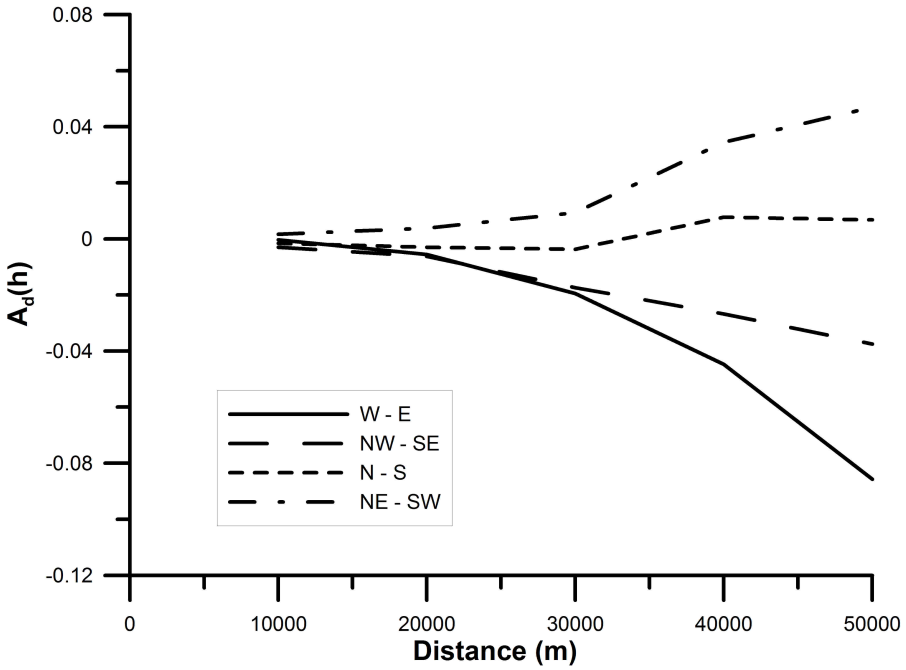

Fig. 16 Asymmetry functions $A_d(h)$ for four selected directions calculated from 175 daily precipitation values measured on January 10, 1993.

ulation based on a convection-resolving model, were used to demonstrate that these processes lead to detectable directional dependencies of the resulting field. The former example was artificially sampled at irregularly spaced locations to demonstrate that the direction-dependent asymmetry obtained using the sampled data is comparable to the one obtained using the dense grid.

Observed topography data from the desert (influenced by wind) and daily precipitation measured at discrete locations show that directional dependencies occurs in real life systems. The latter example demonstrates that a complete image is not required to recognize directional dependence, an unevenly spaced sparse network can also be used to detect it.

Recalling the main research questions of this paper: Can the signs of an irreversible generating processe be detected from a single spatial realization? Is a limited number of irregularly spaced observations sufficient to recognize

the traces of an irreversible process? We can confidently say that both questions can be answered in the affirmative. Using the newly introduced concept of directional dependence for spatial fields in conjunction with the direction-dependent asymmetry function, the signs of an irreversible advective generating process can be detected from a single spatial realization, which can be either a complete dense grid or observations sampled at irregularly spaced locations.

In this paper a very simple possibility of directional dependence was investigated, namely one with a homogeneous direction. Natural processes may have complex directional generating mechanisms which correspond to $v(x)$ field of vectors. In this case the directional asymmetry can be defined as:

$$E\left[(U(x+\alpha v(x))-U(x))^3\right] = A_d(\alpha) \tag{17}$$

The appropriate choice of the vector field and the consideration of it for interpolation and simulation requires further research.

This contribution provides means to recognize directional dependence. Models, simulation and interpolation methods reflecting this kind of dependence remain to be developed to profit from this property.

Acknowledgements Research for this paper was supported by the German Science Foundation (DFG) in the framework of the International Research Training Group NUPUS under grant number GRK 1398.

All data and all results can be requested via email: sebastian.hoerning@iws.uni-stuttgart.de

References

Balmforth N, Provenzale A (eds) (2001) Geomorphological Fluid Mechanics, Springer

Ban N, Schmidli J, Schär C (2014) Evaluation of the convection-resolving regional climate modelling approach in decade-long simulations. Journal of Geophysical Research: Atmospheres 119:7889–7907

Ban N, Schmidli J, Schär C (2015) Heavy precipitation in a changing climate: Does short-term summer precipitation increase faster? Geophysical Research Letters 42:1165–1172

Bárdossy A (2006) Copula-based geostatistical models for groundwater quality parameters. Water Resources Research 42(W11416):doi:10.1029/2005WR004,754

Giannakis G, Tsatsanis M (1994) Time-domain tests for gaussianity and time-reversibility. Signal Processing, IEEE Transactions on 42(12):3460–3472

Guthke P (2013) Non-multi Gaussian spatial structures: Process-driven natural genesis, manifestation, modeling approaches, and influences on dependent processes. Eigenverlag des Instituts Wasserbau

Guthke P, Bárdossy A (2012) Reducing the number of {MC} runs with antithetic and common random fields. Advances in Water Resources 43:1 – 13, DOI http://dx.doi.org/10.1016/j.advwatres.2012.03.014, URL http://www.sciencedirect.com/science/article/pii/S0309170812000693

Haslauer C, Guthke P, Bárdossy A, Sudicky E (2012) Effects of non-gaussian copula-based hydraulic conductivity fields on macrodispersion. Water Resources Research 48(7)

Journel AG, Deutsch CV (1997) Rank order geostatistics: a proposal for a unique coding and common processing of diverse data. in e. y. baafi and n. a. schoolfield (eds.). Geostatistics Wollongong pp 174–187

Lawrance AJ (1991) Directionality and reversibility in time series. International Statistical Review 59(1):67–79

Lawrance AJ, Lewis PAW (1985) Modelling and residual analysis of nonlinear autoregressive time series in exponential variables. Journal of the Royal Statistical Society 47(2):165–202

Nelson R (1999) An Introduction to Copulas. Springer Verlag

Ravalec ML, Noetinger B, Hu LY (2000) The fft moving average (fft-ma) generator: An efficient numerical method for generating and conditioning gaussian simulations. Mathematical Geology 32(6)

Sklar A (1959) Fonctions de répartition à n dimensions et leurs marges. Publ Inst Stat Paris 8:229–131

Steuber TL, Kiessler PC, Lund R (2012) Testing for reversibility in markov chain data. Probability in the Engineering and Informational Sciences 26:593–611

Tsoar H (2001) Types of aeolin sand dunes and their formation. In: Balmforth and Provenzale (2001), pp 403–429

Wood A (1995) When is a truncated covariance function on the line a covariance function on the circle? Statistics & Probability Letters 24:157–164

Wood A, Chan G (1994) Simulation of stationary gaussian process in $[0,1]^d$. Journal Computational and Graphical Statistics 3:409–432

Zinn B, Harvey C (2003) When good statistical models of aquifer heterogeneity go bad: A comparison of flow, dispersion, and mass transfer in connected and multivariate gaussian hydraulic conductivity fields. Water Resour Res 39